Cell

The Neuronal Channel NALCN Contributes Resting Sodium Permeability and Is Required for Normal Respiratory Rhythm

Boxun Lu,[1] Yanhua Su,[1] Sudipto Das,[1] Jin Liu,[1] Jingsheng Xia,[1] and Dejian Ren[1,*]
[1] Department of Biology, University of Pennsylvania, Philadelphia, PA 19104, USA
*Correspondence: dren@sas.upenn.edu
DOI 10.1016/j.cell.2007.02.041

SUMMARY

Sodium plays a key role in determining the basal excitability of the nervous systems through the resting "leak" Na^+ permeabilities, but the molecular identities of the TTX- and Cs^+-resistant Na^+ leak conductance are totally unknown. Here we show that this conductance is formed by the protein NALCN, a substantially uncharacterized member of the sodium/calcium channel family. Unlike any of the other 20 family members, NALCN forms a voltage-independent, nonselective cation channel. NALCN mutant mice have a severely disrupted respiratory rhythm and die within 24 hours of birth. Brain stem-spinal cord recordings reveal reduced neuronal firing. The TTX- and Cs^+-resistant background Na^+ leak current is absent in the mutant hippocampal neurons. The resting membrane potentials of the mutant neurons are relatively insensitive to changes in extracellular Na^+ concentration. Thus, NALCN, a nonselective cation channel, forms the background Na^+ leak conductance and controls neuronal excitability.

INTRODUCTION

The resting membrane potential (RMP) of most mammalian neurons is in the range from −50 to −80 mV, considerably depolarized to the potassium equilibrium potential near −92 mV. This suggests that in addition to resting potassium conductances, there are also conductances due to other ions. In fact, recordings from a variety of neurons reveal a significant resting or background sodium permeability (Hodgkin and Katz, 1949; Nicholls et al., 2001). However, the molecular basis of resting sodium permeability remains unclear. In some neurons, there is resting permeability from hyperpolarization-activated cation channels (I_h, encoded by HCN genes; Robinson and Siegelbaum [2003]), and there can also be resting sodium permeability from TTX-sensitive sodium channels giving a subthreshold, persistent sodium current (Crill, 1996). However, both of these conductances are highly sensitive to voltage, and there is also evidence for a true voltage-insensitive background leak sodium permeability not blocked by Cs or TTX. The leak Na^+ current ($I_{L\text{-}Na}$) is believed to play important roles in the regulation of neuronal excitability, but the in vivo function of such a leak conductance has not been tested because of a lack of specific blockers (Atherton and Bevan, 2005; Eggermann et al., 2003; Hille, 2001; Jackson et al., 2004; Jones, 1989; Nicholls et al., 2001; Pena and Ramirez, 2004; Raman et al., 2000; Robinson and Siegelbaum, 2003). Furthermore, the molecular basis for the voltage-independent sodium permeability is completely unknown.

In animals, voltage-gated Na^+ (Na_V) and Ca^{2+} (Ca_V)-selective channels have four homologous repeats (domains I–IV) of 6TM-spanning segments (S1–S6) (4x6TM) (Catterall, 2000; Goldin, 2002; Hille, 2001). The selectivity filter is formed by stretches of S5-S6 pore (P) loops contributed by each 6TM domain (Figure 1A) (Catterall, 2000; Doyle et al., 1998; Hille, 2001; Sather and McCleskey, 2003). In Ca_V channels, the calcium selectivity requires acidic amino acids that bind Ca (four glutamate [E] or aspartate [D] residues, one from each of the four homologous repeats; EEEE motif) in the mouth of the pore. Na_V channel selectivity filters are generally DEKA in analogous positions (Heinemann et al., 1992; Kim et al., 1993; Sather and McCleskey, 2003; Tang et al., 1993; Yang et al., 1993) (Figure 1A). One member of the 21 genes encoding 4x6TM family *NALCN* (for sodium leak channel, nonselective; previous name, *VGCNL1*; accession number AAN10255) has not been characterized (Figure 1A) (Lee et al., 1999; Yu and Catterall, 2004). NALCN differs from Na_V and Ca_V channels in that it has fewer positively charged residues (arginine or lysine) in its voltage-sensing S4 segments. Additionally, NALCN has an EEKE motif, a mixture of the EEEE (Ca_V) and DEKA (Na_V) residues, in its predicted selectivity filter (Figure 1A).

NALCN is highly conserved in mammals (99% identity between human and rat). *Drosophila melanogaster* has a NALCN homology named α1U (for unusual α1 subunit, accession number AY160083, 57% identity with the human homolog) (Littleton and Ganetzky, 2000). Hypomorphic

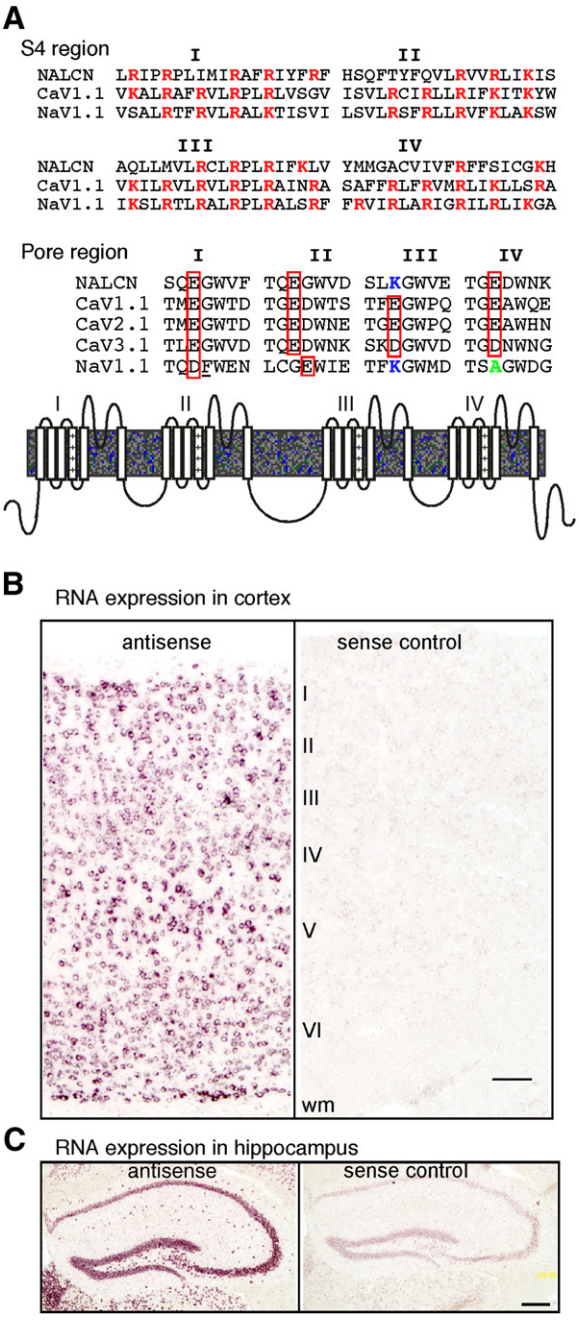

Figure 1. NALCN Is Widely Expressed in the Central Nervous System

(A) Alignment of the S4 and pore regions between NALCN, representative Ca_V and Na_V channels. Schematic drawing illustrates that the Ca_V and Na_V pore-forming subunits (α1) are composed of four homologous repeats (I, II, III, IV). The EEEE (DEKA) motifs in Ca^{2+} (Na^+) channel pore regions are highlighted. A key aromatic residue (F) in $Na_V1.1$ important for Na_V's TTX sensitivity is underlined.

(B and C) In situ staining with slices from cerebral cortex (B) and hippocampus (C). The gray matter (I-VI) and white matter (wm) layers in the cortex are indicated (B). Scale bar, 100 μm in (B) and 250 μM in (C). Sense RNA probes (right panels) are used as negative control for signal specificity.

alleles in the fruit flies with reduced NALCN expression, although viable and fertile, have altered locomotive behavioral circadian rhythms (Lear et al., 2005; Nash et al., 2002). Furthermore, the mutant flies display a narrow abdomen phenotype (*na*) and have altered sensitivities to general anesthetics such as halothane (Krishnan and Nash, 1990; Mir et al., 1997; van Swinderen, 2006). Two homologs also exist in *C. elegans* (nca-1, accession number NP_741413; nca-2, accession number NP_498054; both with 48% identity to the human homolog). The functional significance of NALCN in mammals and whether NALCN indeed encodes a plasma membrane ion channel are unknown (Lee et al., 1999).

Here we report that NALCN forms a voltage-independent, nonselective, noninactivating cation channel permeable to Na^+, K^+, and Ca^{2+}. Mice with deletion of the *NALCN* gene have a severely disrupted respiratory rhythm characterized by a regular rhythm interrupted by periods of apnea. Mutant pups die within 24 hr of birth. Hippocampal neurons from the mutant lack $I_{L\text{-}Na}$ and the current can be restored by NALCN cDNA transfection. We thus conclude that NALCN, a nonselective cation channel, encodes the neuronal background Na^+ leak conductance.

RESULTS

Expression of NALCN in Central Nervous System Neurons

Northern blot analysis suggested that NALCN mRNA is expressed in all brain regions (Lee et al., 1999). To determine which types of cells express the gene, we carried out in situ hybridization of mouse brain slices with DIG-labeled RNA probes derived from its 1.8 kb cDNA (carboxyl terminus). In the cerebral cortex (Figure 1B) and hippocampus (Figure 1C), an antisense RNA probe detected NALCN mRNA expression in all layers and in essentially all the neurons. Sense RNA probe was minimally detected, demonstrating specificity of staining. Similarly, NALCN mRNA was detected in all neurons of the spinal cord dorsal and ventral horns (data not shown). Using northern blot and in situ hybridization, we did not detect NALCN expression in liver, muscle, lung, kidney, or testis (data not shown, see also Lee et al. [1999]). These experiments suggest that NALCN is likely a widely expressed neuronal ion channel.

NALCN Is a Voltage-Independent Ion Channel

Attempts to functionally reconstitute NALCN as an ion channel in heterologous systems have been unsuccessful (Lear et al., 2005; Lee et al., 1999; Yu and Catterall, 2004). To determine if NALCN indeed encodes an ion channel, we transfected NALCN-encoding cDNA into HEK293 cells and recorded whole-cell current 48–72 hr after transfection (Figure 2A). Immediately after break-in, >80% (19 of 22) of NALCN-transfected cells appeared "leaky," had input resistance below 1 GΩ, and displayed a current with a linear current-voltage (I-V) relationship (I_{NALCN}, −22 to −1691 pA; −573 ± 124 pA, at −80 mV; n = 22) that was largely absent in mock-transfected (−10 ± 3 pA, n = 15)

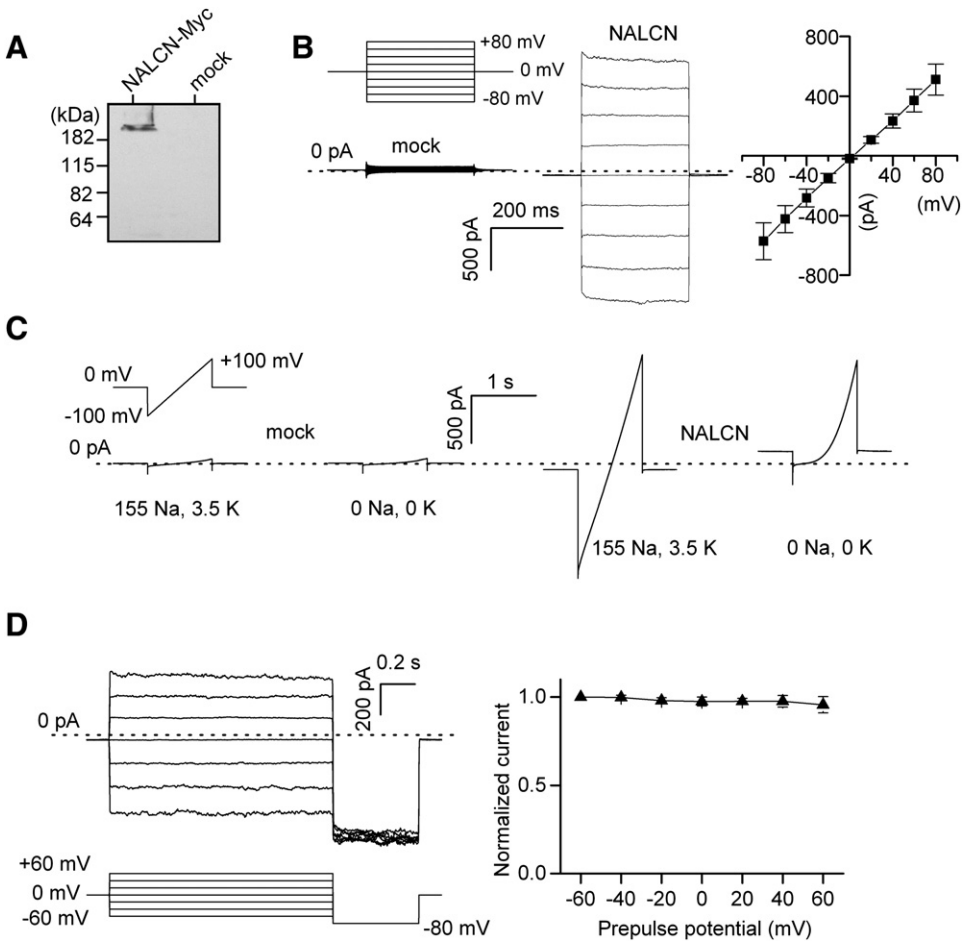

Figure 2. NALCN Forms a Voltage-Independent Ion Channel

(A) Expression of myc-tagged NALCN protein (detected using Western blot analysis with anti-myc antibody).

(B) Representative current traces elicited by step voltage protocols (upper left) from mock- (lower left) and NALCN- (middle) transfected cells. (Right) Averaged current-voltage (I-V) relationship showing voltage-independent activation of NALCN (n = 22).

(C) Currents elicited by a voltage ramp protocol (from −100 mV to +100 mV in one second, upper left) in bath with (155 Na, 3.5 K) or without (0 Na, 0 K) K^+ and Na^+. Representative recordings from one mock transfected (left two panels) and one NALCN transfected (right two panels) are shown.

(D) Lack of inactivation of I_{NALCN}. (Upper left) Representative current traces. (Lower left) Protocol, (right) normalized currents at −80 mV following prepulses of various voltages. Dotted lines indicate zero current level. Data are represented as mean ± SEM. All experiments were performed using HEK293 cells except that COS-7 cells were used for the protein work in (A).

and nontransfected control cells (Figure 2B). Since currents with a linear I-V curve (Figure 2B) could also be generated by nonspecific leaks from cell damage or through poor seals, we used ion replacement to ensure that the currents analyzed were from ion-selective conductances. When extracellular Na^+ and K^+ were replaced with larger ions $Tris^+$ or $NMDG^+$, the inward currents were largely abolished and the I-V curves became outwardly rectifying (Figure 2C). The input resistance (R_m) under this condition became >1 GΩ (at −80 mV). I_{NALCN} could also be suppressed by channel blockers (see below).

Unlike the ten Ca_V and nine Na_V members in the 4x6TM channel family, NALCN's activation is voltage independent (Figure 2B). No significant voltage-dependent inactivation was observed (Figures 2C and 2D). The lack of voltage dependence of activation and inactivation is likely a result of the absence of some of the charged residues conserved in the S4 domains of voltage-gated channels (Figure 1A) (Bezanilla, 2000; Hille, 2001; Horn, 2002).

NALCN Is Nonselective, Permeable to Na^+, K^+, and Ca^{2+}

Replacement of >90% of Cl^- in the bath by methanesulfonate (MES) did not result in a significant change in the size or reversal potential of the current (Figure 3A), indicating that NALCN was impermeable to anion and that the current was carried by cations. In contrast, changing $[Na^+]_o$ from 155 to 15.5 mM reduced the amplitude of inward current and shifted the reversal potential, suggesting Na^+ as a permeant ion (Figure 3B). NALCN is also clearly

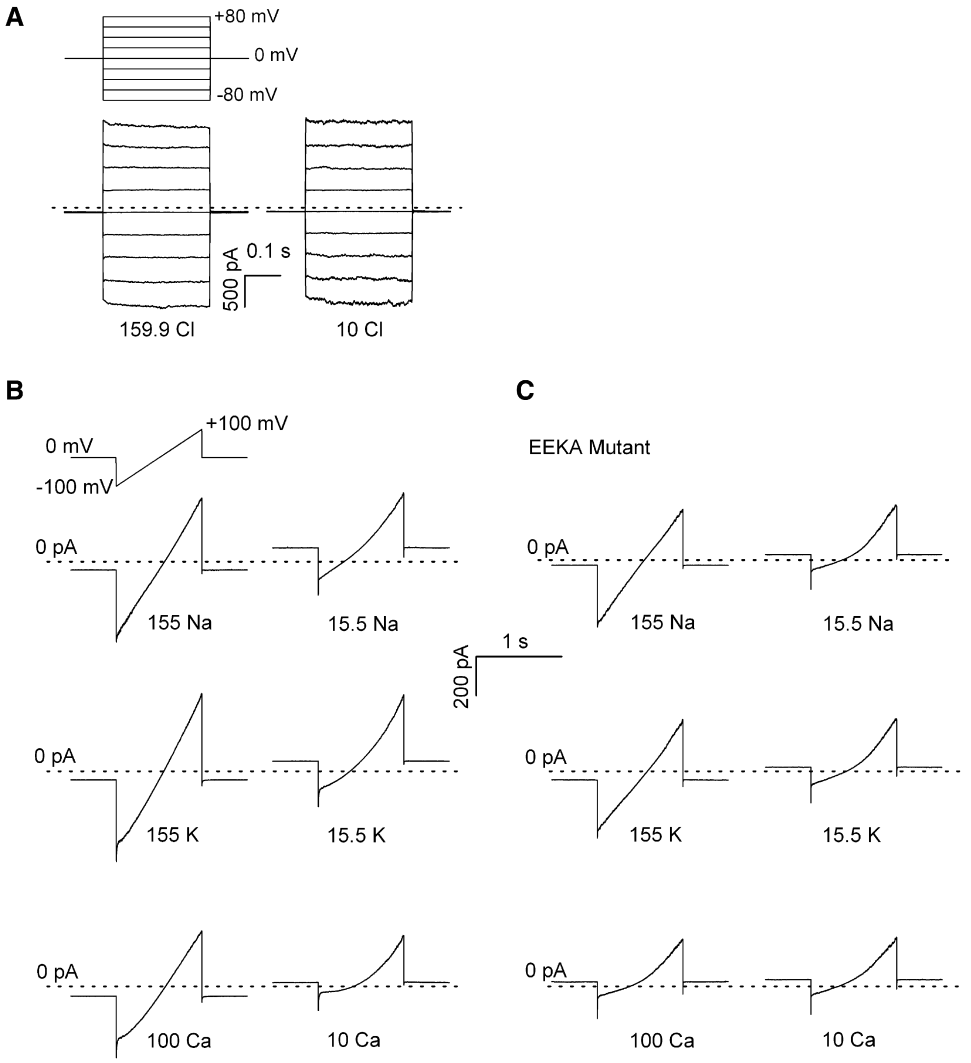

Figure 3. NALCN Is a Nonselective Cation Channel

(A) Representative currents recorded in bath with high (159.9 mM, left) and low (10 mM, right) [Cl^-] using a step protocol (−80 mV to 80 mV in steps of 20 mV; Vh = 0 mV; upper panel).

(B) Currents from a representative NALCN-transfected cell in bi-ionic conditions with extracellular cation concentrations as indicated. NMDG was used to partially replace the cation in low-cation concentration baths (15.5 Na, 15.5 K or 10 Ca). A ramp protocol (Vh = 0 mV, from −100 mV to 100 mV in 1 s; upper left) was used.

(C) Similar to (B) but from a cell transfected with an EEKA mutant NALCN channel with E1389 (in repeat IV, Figure 1A) mutated to A using site-directed mutagenesis.

permeable to K^+ and Ca^{2+} (Figure 3B). We used reversal potentials of I_{NALCN} under various bi-ionic conditions to estimate the ion selectivity of the channel. The selectivity sequence was P_{Na} (1.3, n = 12) > P_K (1.2, n = 5) > P_{Cs} (1.0, n = 12) > P_{Ca} (0.5, n = 7). Thus, NALCN is a nonselective cation channel, unlike any of the other 20 members in the 4x6TM channel family, which are highly selective for either Na^+ (Na_V1-9 and Na_X) or Ca^{2+} ($Ca_V1.1$-1.4, $Ca_V2.1$-2.3, and $Ca_V3.1$-3.3) (Yu and Catterall, 2004). The channel's unique ion selectivity is likely the result of its unusual sequences of amino acids associated with the putative channel pore (Figure 1A), as suggested by the extensive mutagenesis studies carried out on the EEEE motif in Ca_Vs and DEKA in Na_Vs (Heinemann et al., 1992; Kim et al., 1993; Sather and McCleskey, 2003; Tang et al., 1993; Yang et al., 1993). In support of the importance of the EEKE motif in NALCN's ion selectivity, a mutant NALCN with an EEKA motif had a largely decreased Ca^{2+} permeability; P_{Na} (1.3, n = 11) = P_K (1.3, n = 8) > P_{Cs} (1.0, n = 11) > P_{Ca} (0.1, n = 11) (Figure 3C). The involvement of amino acids surrounding the EEKE locus (Figure 1A) in ion selectivity may explain why the EEKA mutant is not as Na^+ selective as Na_V channels (DEKA motif).

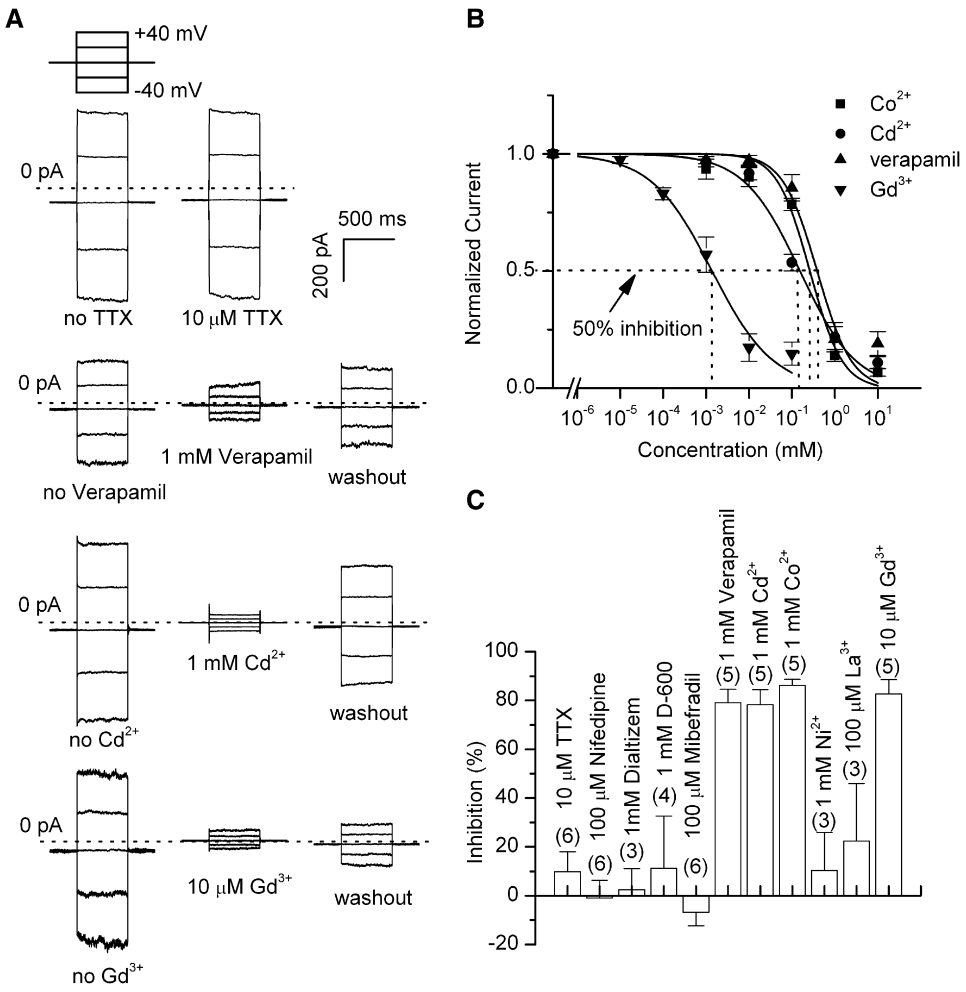

Figure 4. Sensitivities of I_{NALCN} to Divalent Ions, Trivalent Ions, and Na_V and Ca_V Blockers

(A) Representative sensitivities of I_{NALCN} to blockade by TTX, verapamil, Cd^{2+}, and Gd^{3+}. A step protocol (−40 mV to 40 mV in step of 20 mV; 500 ms; Vh = 0 mV; upper) was used.

(B) Inhibition curves showing apparent IC_{50}s. The curves were reconstructed using the current sizes at −80 mV obtained with a ramp protocol (n = 5).

(C) Percentage of inhibitions of the current by various blockers of indicated concentrations. Numbers of cells tested are in parentheses. Data are represented as mean ± SEM.

I_{NALCN} was not blocked by the Na_V channel blocker TTX (up to 10 μM) (Figures 4A and 4C) but could be partially blocked by several Ca_V blockers with low affinity (apparent IC_{50}s, 0.15 mM for Cd^{2+}, 0.26 mM for Co^{2+}, and 0.38 mM for verapamil) (Figure 4B). The trivalent ion Gd^{3+}, which is often considered a high-affinity blocker for stretch-activated channels (Yang and Sachs, 1989), effectively blocked I_{NALCN} with an apparent IC_{50} of 1.4 μM (Figure 4). The overall properties of I_{NALCN} (including the I-V relationship, activation, inactivation, P_{Ca}/P_{Na}, and pharmacology) are unlike those of the majority of TRP cation channels, making it unlikely that the currents we recorded were through nonspecific leaks or through other proteins such as TRPs that could have been upregulated by the NALCN cDNA transfection (see the Experimental Procedures for details).

Neonatal Lethality and Respiratory Rhythm Defects Caused by Targeted Disruption of the *NALCN* Gene

To uncover the in vivo function of NALCN, we generated mice with *NALCN*'s exon 1 deleted (Figure 5A). Semiquantitative RT-PCR assays show that the homozygous mutant (E18.5 embryos) did not express the wild-type (WT) NALCN mRNA; heterozygotes expressed reduced amounts in brain (Figure 5A). Mice were born in a roughly Mendelian ratio (22% −/−, 27% +/+ and 51% +/−; from 1043 pups in 127 litters, tail clips used for genotyping collected within ~10 hr of birth), suggesting that the channel gene is not required for embryonic viability. We did not observe gross differences in embryonic development, righting responses, spontaneous limb movement, and toe/tail pinch responses between WT and mutant newborn pups. The homozygous mutants appeared normal up to 12 hr

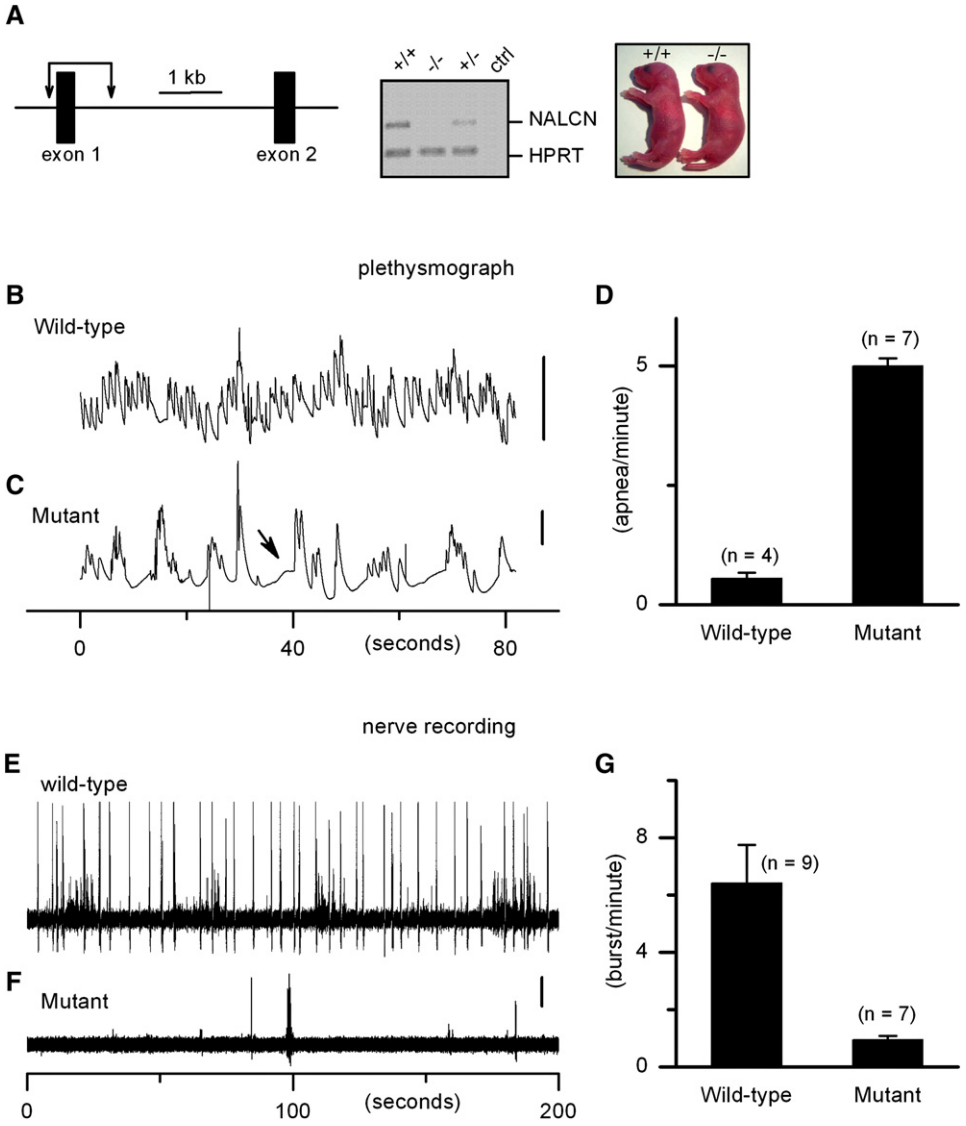

Figure 5. NALCN Is Required for Normal Respiratory Rhythm and Neonatal Survival

(A) Targeted disruption of *NALCN*. (Left) Partial genomic structure in the region containing exons 1 and 2. Connected arrows mark the deletion in the mutant. (Middle) Semiquantitive RT-PCR using brain RNAs from E18.5 embryos with various genotypes. NALCN primers amplify 479 bp. A primer pair amplifying a housekeeping gene (HPRT) was also included as internal control. RT reaction without reverse transcriptase was used as template in the PCR negative control ("ctrl" lane). (Right) Representative appearances of newborn WT (+/+) and mutant (−/−) pups.

(B–G) Respiratory rhythm defects in the mutant, as measured by plethysmograph (B–D) and C4 nerve root recordings from brain stem spinal cord preparations (E–G). Plethysmograph detected regular rhythmic respiratory activities in the WT P0 pups (B), but the rhythm was disrupted in the mutant (C). The mutant pups displayed periodic apnea (indicated by the arrow in [C]; defined as the absence of inspiration for longer than 3 s) (D). C4 nerve root recordings detected rhythmic electrical activities in the WT (E), but the burst activities were nearly absent in the mutant (F and G). Scale bars, 5 μl for (B) and (C); 50 μV for (E) and (F). Data are represented as the mean ± SEM.

after birth (Figure 5A). No mutant, however, survived beyond 24 hr after birth (data from 52 mutant pups in 28 litters). Thus, NALCN is one of the few channels in the 4x6TM channel family required for neonatal survival.

A clear distinction between null and WT mouse breathing patterns was apparent. Null mice respiration was sporadic, with apnea for a few seconds before beginning a burst of deep breathing lasting 5–10 s (data from >20 pairs). We measured the respiratory patterns using a whole-body plethysmograph, which detected the pressure changes generated by the breathing activities of the mice. The WT and mutant pups were subjected to recording a few hours after they were born, when they appeared otherwise indistinguishable. WT mice breathed in a well-defined rhythm (Figure 5B). Null mice breathing was characterized by apnea for ~5 s followed by a burst of

breathing of ~5 s, at a rate of ~5 apnea events/minute (Figures 5C and 5D). Intriguingly, this pattern is reminiscent of the periodic breathing of Cheyne-Stokes respiration found in humans with CNS damage (Strohl, 2003).

Respiratory rhythms are controlled by the central nervous system. Given the expression of the NALCN channel in CNS neurons but absence in muscle, and the ability of the mutant pups to breathe, we suspected that the disrupted respiratory patterns in the mutant was due to a defect in neuronal control. We recorded the electrical activities from the fourth cervical nerve root (C4) that innervates the diaphragm and discharges rhythmic electrical signals that regulate breathing. The C4 nerves in isolated brain stem spinal cords from newborn pups (P0) have robust rhythmic electrical activities in WT mice (Figures 5E and 5G). In null mice, however, such electrical activities were largely absent (Figures 5F and 5G). These recordings support the hypothesis that severe defects in the respiratory rhythm in the null mice were due to defects in electrical signaling in the nervous system.

NALCN Encodes the Cs^+- and TTX-Resistant Background Na^+ Conductance in Neurons

To determine the native channel that NALCN encodes, we measured currents in hippocampal neurons that express NALCN mRNA and are among the best electrically characterized neurons (Figure 1C). Using a slow ramp protocol, the TTX-sensitive, persistent Na^+ current was observed in both WT and mutant mice (data not shown) (Raman and Bean, 1997). In addition, we used step protocols to record the Na_V and Ca_V currents. The Na_V current density in the mutant was not significantly different from the WT (WT, −26.0 ± 7.1 pA/pF, n = 10; mutant, −25.3 ± 7.0 pA/pF, n = 10; at −17 mV). We next examined the Ca_V currents using Ba^{2+} as the charge carrier. Ba^{2+} currents elicited in the mutant and WT neurons were comparable (WT, −35.1 ± 6.0 pA/pF, n = 5; mutant, −25.7 ± 8.2 pA/pF, n = 5; at −10 mV). Consistent with this observation, depolarization with 40 mM $[K^+]_o$ readily evoked $[Ca^{2+}]_i$ increases in both WT and mutant neurons when assayed with Fura-2 Ca^{2+} imaging (data not shown). Thus, the disruption in *NALCN* likely did not lead to nonspecific effects on Na_V or Ca_V channels.

NALCN expressed in HEK293 cells has a linear I-V relationship, is permeable to Na^+, and is constitutively open (Figures 2 and 3). These properties fit reasonably well with those of $I_{L\text{-}Na}$ (Nicholls et al., 2001). To compare the Na^+ leak currents in hippocampal neurons cultured from WT and the mutant, we used extracellular baths containing TTX (1 μM) and Cs^+ (2 mM) to block the Na_v and I_h currents, respectively. The small $I_{L\text{-}Na}$ leak current was further isolated by subtracting the currents recorded in low (14 mM) $[Na^+]_o$ from those in high (140 mM) $[Na^+]_o$ at holding potentials ($\Delta I_{L\text{-}Na}$ at −68 mV) (Raman et al., 2000; Simasko, 1994) (Figure 6A) (see the Experimental Procedures). In WT neurons, 97% (29 of 30) had $\Delta I_{L\text{-}Na}$ larger than 5 pA (−13.2 ± 0.8 pA at −68 mV, n = 30). In contrast, none of the 15 mutant neurons measured had $\Delta I_{L\text{-}Na}$ >5 pA (−0.2 ± 0.7 pA) within the resolution limit of our measurement (Figures 6A and 6B). Transfection of NALCN to the mutant neurons restored and enhanced the Na^+ current ($\Delta I_{L\text{-}Na}$, −72.4 ± 14.4 pA, n = 12) (Figures 6A and 6B), while transfection of an empty vector failed to do so (Figure 6B). Taken together, these data suggest that the TTX- and Cs^+-insensitive background Na^+ leak current $I_{L\text{-}Na}$ is likely carried by the nonselective NALCN-containing channel.

Hypothetically, $I_{L\text{-}Na}$ would balance background K^+ currents to maintain the RMP and regulate neuronal excitability (Hille, 2001; Nicholls et al., 2001). Consistent with this notion, the mutant neurons were hyperpolarized (RMP, −71.4 ± 3.2 mV, n = 14) compared with WT (−61.3 ± 1.2 mV, n = 24) (Figure 6C). Furthermore, mutant neurons were markedly depolarized when transfected with NALCN cDNA (−36.5 ± 3.7 mV, n = 15), but not with empty vector (−67.9 ± 3.0 mV, n = 5) (Figure 6C).

To test if the NALCN-encoded channel contributes to the sensitivity of the neuron's membrane potential to extracellular $[Na^+]$, we monitored MPs while $[Na^+]_o$ was reduced. A drop of $[Na^+]_o$ from 140 mM to 14 mM led to a hyperpolarization (ΔVm, −13.7 ± 1.6 mV, n = 17) in the WT neurons. In contrast, such effect of a 10-fold $[Na^+]_o$ drop was largely diminished in the mutant (ΔVm, −3.1 ± 1.5 mV, n = 10) (Figures 6D and 6E). Transfection of NALCN cDNA to the mutant neurons restored and enhanced the sensitivity (ΔVm, −32.0 ± 2.9 mV, n = 9), while transfection with an empty vector did not have a similar effect (ΔVm, 0.0 ± 0.8 mV, n = 5) (Figures 6D and 6E).

NALCN Regulates Neuronal Excitability

In addition to the NALCN channel carrying the Cs^+- and TTX-insensitive Na^+ leak (Figure 6B), Na_V (activated by depolarization, blocked by TTX) and I_h (activated by hyperpolarization, blocked by Cs^+) may be partially active and may serve as two additional paths for the total Na^+ leak at RMPs in mammalian neurons (*C. elegans* has two NALCN genes but no genes encoding Na_V or I_h) (Nicholls et al., 2001). To determine the relative contribution of each of the three components, we measured $\Delta I_{L\text{-}Na}$ in the same neuron in the absence of TTX and Cs^+, in the presence of Cs^+, and in the presence of both TTX and Cs^+. The relative contributions of I_{NALCN}, I_h and Na_V to the total background Na^+ current were estimated to be 72.1% ± 4.1%, 9.6% ± 11.5%, and 18.3% ± 10.9% (n = 5), respectively (Figure 7A). These data suggest NALCN channel as the dominant path for the Na^+ leak in the hippocampal neurons. Consistent with the major contribution of NALCN, mutant neurons' MPs are relatively insensitive to the change of $[Na^+]_o$, even in the absence of Cs^+ and TTX (Figure 7B).

Finally, we tested if NALCN contributes to neuronal excitability. In WT neurons, the frequency of continuous firing could be significantly reduced by an application of 10 μM Gd^{3+} (77.1% ± 5.3%, n = 7) (Figure 7C, upper panel; Figure 7D). Consistent with the idea that the frequency reduction was due to a blockade of the I_{NALCN} leak current, injection of a depolarizing current restored the firing

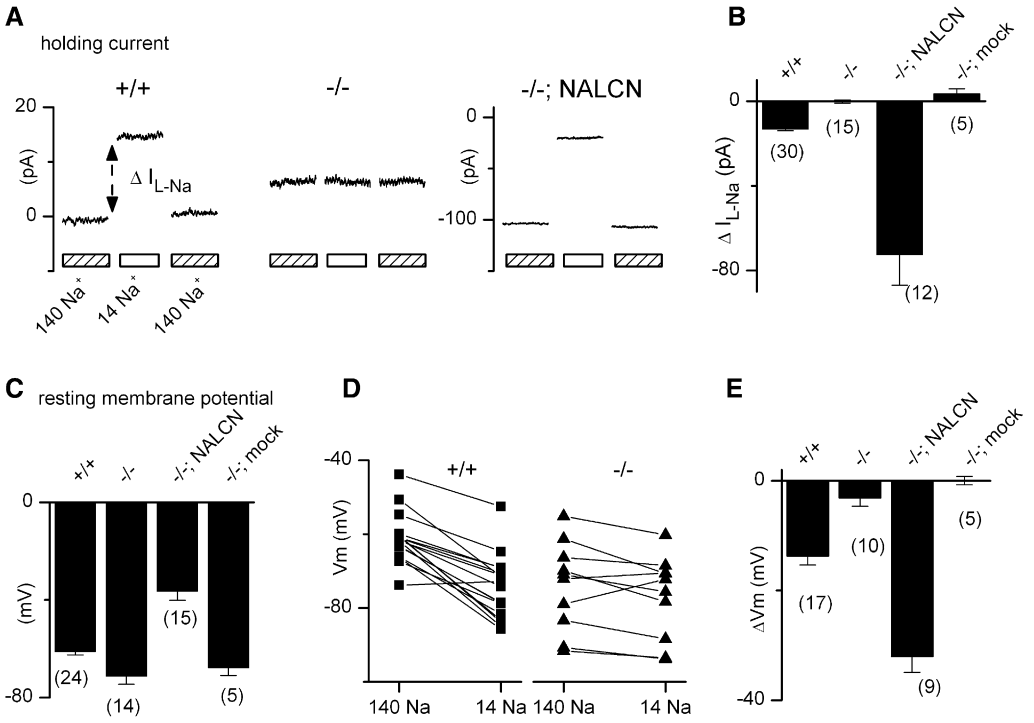

Figure 6. NALCN Encodes the Cs^+- and TTX-Insensitive Sodium Leak Current $I_{L\text{-}Na}$ in Hippocampal Neurons

All recordings were done in the presence of TTX (1 μM) and Cs (2 mM).

(A) Representative holding currents (at −68 mV) in baths containing 140 mM (indicated by hatched bars) or 14 mM Na^+ (open bars) from a WT (+/+) neuron, a mutant (−/−), and a mutant transfected with NALCN cDNA (−/−; NALCN). $\Delta I_{L\text{-}Na}$ (indicated by double-headed arrow) was calculated as the difference recorded between the 140 mM and 14 mM Na^+-containing baths. Note different scale for the transfected neuron. Recording of 0.25 s is shown for each condition.

(B) Summary of $\Delta I_{L\text{-}Na}$. Numbers of cells tested are given in parentheses.

(C) Averaged RMPs (measured with current clamp).

(D) Changes in membrane potential in the WT and mutant neurons in response to $[Na^+]_o$ change from 140 mM to 14 mM. Each connected line represents an individual neuron. Several lines in the WT (+/+) overlap.

(E) Summary of membrane potential changes upon the $[Na^+]_o$ drop. Data are represented as mean ± SEM.

frequency. This blockade effect of 10 μM Gd^{3+} was largely absent in the mutant neurons (10.6% ± 5.8%, n = 8) (Figure 7C, lower panel; Figure 7D). Similarly, application of another NALCN blocker, verapamil (0.5 mM), reduced the firing frequency in the WT neurons (84.4% ± 4.4%, n = 11) but had less effect in the mutant (22.2% ± 11.9%, n = 7) (Figure 7D). The residual effect of verapamil in the mutant was likely due to its action on other targets such as Ca_V channels.

DISCUSSION

Unlike any of the other 20 members in the 4x6TM channel family, NALCN forms a voltage- independent, nonselective, noninactivating cation channel. The Cs^+- and TTX-insensitive background Na^+ leak current is absent in NALCN mutant neurons and can be restored by transient expression of NALCN using cDNA transfection. The sensitivity of the RMP to $[Na^+]_o$ changes is largely diminished in the mutant. Finally, blockers that suppress I_{NALCN} had little effect on the mutant neurons' excitability. The simplest interpretation of our work is that NALCN encodes a cation-nonselective, voltage-insensitive channel that is responsible for the background Na^+ leak current ($I_{L\text{-}Na}$) in neurons and is indispensable for neonatal survival. The 21 mammalian members in the four-repeat (4x6TM) ion channel family can now be functionally divided into three subfamilies of Ca^{2+} channels (ten members), Na^+ channels (ten members), and nonselective cation channel (one member).

In the NALCN-deficient mice, spinal cord nerves (C4) lack the rhythmic electrical discharge that affects respiratory behavior. Invertebrates do not have analogous spinal cord nerves, but the defects in locomotive behavioral circadian rhythms in the *Drosophila* mutant with reduced NALCN expression point to the possibility that a common function of the channel is in neuronal rhythm generation and/or coordination (Lear et al., 2005; Nash et al., 2002; Robinson and Siegelbaum, 2003). Alternatively, as the channel is widely expressed in the nervous systems, a global reduction of excitability in the mutant may lead to the disruption in respiration (Feldman et al., 2003). The exact causes of the neonatal fatality need to be further

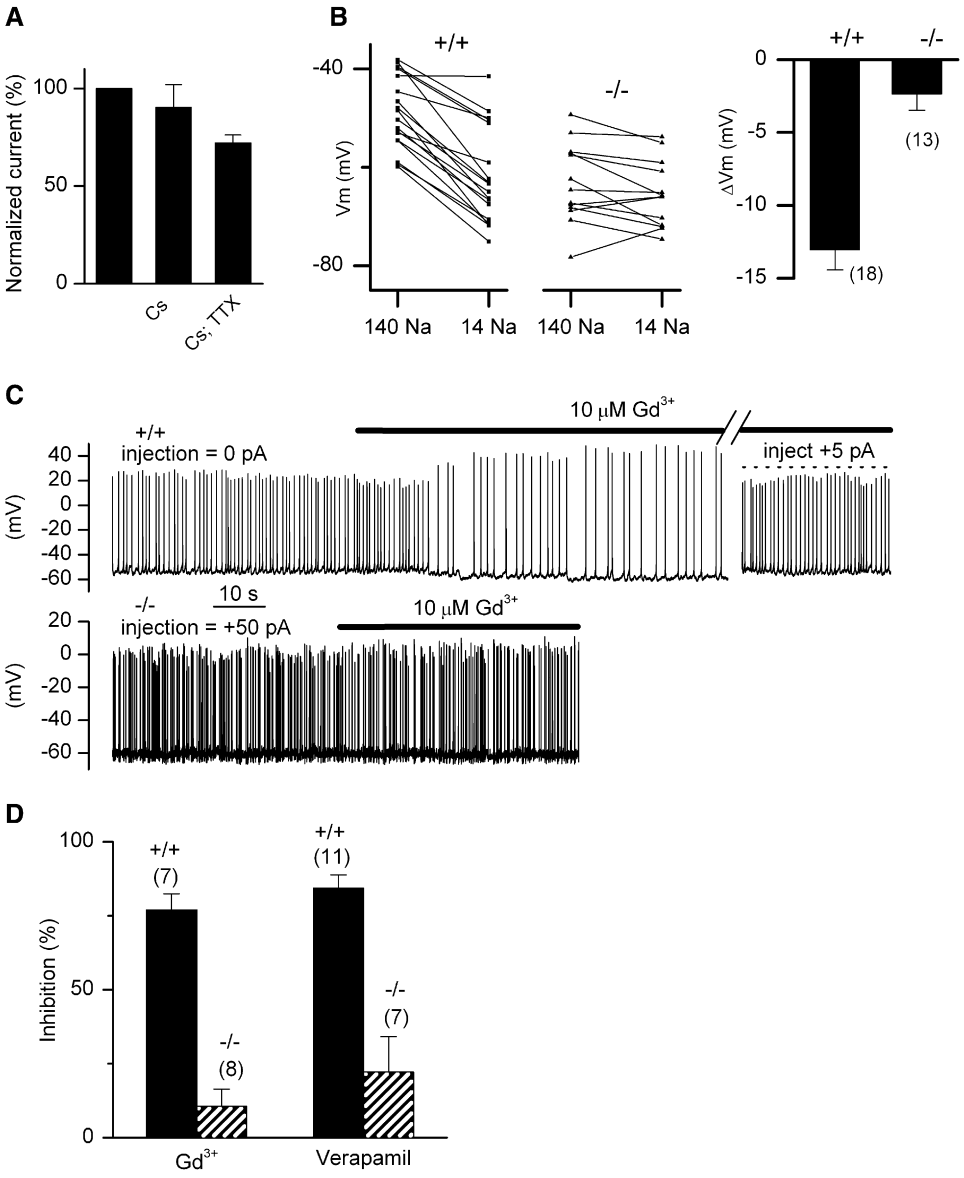

Figure 7. NALCN Is a Major Determinant of the Total Background Na^+ Currents and Controls Neuronal Excitability

(A) Background Na^+ currents ($\Delta I_{L\text{-}Na}$ at −68 mV; WT neurons) in baths without Cs^+ and TTX, with Cs^+ alone (2 mM), or with both Cs^+ and TTX (1 μM). The currents were normalized to that measured in baths without Cs^+ and TTX. Note that the TTX- and Cs-insensitive component (72% of total) was abolished in the NALCN mutant (Figure 5).

(B) Changes in membrane potential in the WT and mutant neurons in response to $[Na^+]_o$ change, in the absence of Cs^+ and TTX. Right panel gives the averaged changes.

(C) Representative effects on action potential firing frequency of 10 μM Gd^{3+} in a WT (upper, no current injection) and mutant (lower, continuous firing elicited by a +50 pA current injection) neuron. In the WT, the blockade could be "rescued" by injecting a depolarizing current (+5 pA). Note a hyperpolarization of baseline membrane potential by Gd^{3+} in the WT, but not in the mutant.

(D) Summary of percentage reductions of firing frequency in the WT and mutant by Gd^{3+} (10 μM) or verapamil (0.5 mM). Data are represented as mean ± SEM.

investigated. In addition to the defect in behavioral circadian rhythms, the *Drosophila* mutant also displays other phenotypes, including narrow abdomen and altered sensitivity to anesthetics (Krishnan and Nash, 1990; Mir et al., 1997; van Swinderen, 2006). The complexity of the phenotypes suggests additional physiological roles of the NALCN channel. A conditional knockout mouse model will be able to address the roles of NALCN in adults. In *C. elegans*, the action potential is clearly Na^+ dependent (Franks et al., 2002). In contrast to mammals, the worm genome does not appear to contain genes encoding Na_V or I_h (Bargmann, 1998; Robinson and Siegelbaum, 2003)

but has two NALCN homologs that could potentially serve as the Na^+ conductances.

Two major background cation leak conductances operate to oppose each other in establishing the RMP in neurons, with the Na^+ leak conductance being normally a fraction (~4% in the squid giant axon) of that of the K^+ conductance (Hodgkin and Katz, 1949; Nicholls et al., 2001). K^+ leak current is likely contributed by many channels, including the 15 K^+ channels in the K2P family (Goldstein et al., 2005). In support of this redundancy, none of the two K2P channel knockouts (KCNK2 and KCNK4) was shown to lead to defects in neuronal excitability or animal survival. Nor was a reduction in background K^+ leak current reported, although the channels overexpressed in heterologous systems clearly showed properties of background K^+ leak conductances (Heurteaux et al., 2004).

Sources of the Na^+ leak conductance have been speculated to be via Na_V channels, nonselective channels, Na^+ leak through K^+ channels, and transporters (Nicholls et al., 2001). Our data suggest that the molecular mechanism for the Na^+ leak is surprisingly simple. In the NALCN mutant neurons, the Na^+ leak is undetectable in the presence of TTX and Cs^+. These results suggest that the Na^+ leak conductance consists of three components: a Cs^+-sensitive (possibly from I_h), a TTX-sensitive (likely from Na_V), and a NALCN-dependent component, with NALCN providing the majority of leak current. In animals without voltage-activated I_h and Na_V, NALCN is likely the sole source for the major Na^+ conductance. Other candidates for leak currents are some members of the 28 mammalian TRP channels that are involved in sensory transduction and activated by receptors and ligands (Ramsey et al., 2006). Most of the TRP currents are nonlinear and reverse at potentials above 0 mV. None of the ten reported TRP subtype knockouts has been reported to lead to defect in the Na^+ leak or neuronal excitability (Nilius et al., 2005). Nevertheless, we cannot exclude the possibility that conductances beyond our detection limit and/or channels that are downregulated in the NALCN mutant but restored and enhanced upon NALCN transient expression also contribute to the leak current.

In summary, NALCN is widely expressed in the brain and spinal cord neurons and forms a major background Na^+ conductance. NALCN channels are nonselective, voltage independent, and do not inactivate. As such, they are ideal for setting levels of neuronal excitability and thus controlling firing rates. Interesting questions for the future are whether their expression or activity can be altered by signal transduction events or neuronal plasticity or are targets for therapeutics.

EXPERIMENTAL PROCEDURES

In Situ Staining

Frozen mouse sections (10 μm thick) were used for in situ staining. A DNA fragment of 1811 bp, starting from nucleotide 4764, was amplified from mouse brain and subcloned into pBlueScript II SK(−) for single-strand, digoxigenin (DIG)-labeled RNA probe synthesis. This fragment has no significant sequence similarity with any other genes in the genome. Sense probe was used as negative control. Hybridizations were washed and signals were visualized using AP-conjugated anti-DIG antibody and BCIP/NBT substrate.

Knockout Mice Generation

Animal uses followed protocols approved by the Institutional Animal Care and Use Committee (IACUC) at the University of Pennsylvania. The targeting vector was generated with pKO NTKV-1903 (Stratagene) as a backbone. The left and right arms have 3 kb and 1.5 kb, respectively. LoxP sites were engineered in the 5′UTR (20 bp from the translational start codon) and 360 bp into the intron following exon 1. A correctly targeted ES cell clone was used to generate chimeric mice. Heterozygous mice were mated to a line expressing CRE recombinase to delete exon 1 flanked by the LoxP sites. Mice used to generate the data were from mating between heterozygous that had been backcrossed to C57BL/6 for three or more generations. Due to a lack of specific antibodies, we have not determined the stability of protein encoded by mutant transcripts. Genomic PCR was used to identify the mutant. For RT-PCR, total RNAs were isolated from E18.5 embryos using the NucleoSpin RNA II Kit (Macherey-Nagel). cDNAs were synthesized using RETROscript Kit (Ambion). The primers amplifying 479 bp of NALCN mRNA span exons 1 and 4, a region containing introns of ~7 kb. The forward and reverse primers have the sequences (5′→3′) ATGCTCAAAAGAAAGCAGAGTTCCA and AATCGGAAATAAATCCT GAAAGCCC, respectively. Primers amplifying a 261 bp fragment of the mouse HPRT gene were included in the same tube and served as an internal control. PCR conditions were the following: 28 cycles composed of 1 min denaturation at 95°C, 1 min primer annealing at 60°C, and 2 min extension at 72°C using 0.05 unit/μl Taq DNA Polymerase (Promega).

Plethysmograph

Plethysmography employed a differential pressure transducer (Omega Engineering, Model PX65, ±0.25% linearity). Data were collected through a digitizer and AxoScope software and band-pass filtered at 0.1 to 500 Hz (Axon). The experiments were performed at 32°C, close to the body temperature of newborn pups.

C4 Nerve Root Recording

C4 nerve recordings using the brain stem-spinal cord preparation followed previously described methods (Di Pasquale et al., 1996; Viemari et al., 2003). The brain stem and cervical spinal cords prepared from P0 pups were superfused with oxygenized (95% O_2/5% CO_2) artificial cerebrospinal fluid containing (in mM) 129 NaCl, 3.35 KCl, 1.26 $CaCl_2$, 1.15 $MgCl_2$, 21.0 $NaHCO_3$, 0.58 NaH_2PO_4, and 30 glucose (pH 7.4). Burst activities recorded from the C4 ventral roots using suction electrodes (40–60 μm opening) were amplified (GeneClamp 500B, Axon), lowpass filtered at 1 kHz, and digitized at 2 kHz using a DigiData 1322A controlled by Clampex 9.2 software. Experiments were performed at ~28°C.

Hippocampal Neuronal Culture

Hippocampi were isolated from P0 pups following genotype identification. Neurons acutely dissociated with protease were used for patch-clamp recordings on the same day (Jackson et al., 2004). For long-term culture, hippocampi were dissected into cold Ca^{2+}- and Mg^{2+}-free Hank's or PBS buffer. Chopped small pieces were digested in solution containing 20 units/ml papain activated by 1 mM cysteine, for 20–30 min at 37°C. Neurons were dissociated by trituration with fire-polished glass pipettes and plated onto polylysine-coated dishes at 4 × 10^5 cell/35 mm dish, or glia-preplated dishes at 2 × 10^5/35 mm dish. The growth medium was composed of 80% DMEM (with 4.5 g/L glucose, 25 mM HEPES, no glutamine), 10% Ham's F-12 (Cambrex), 10% bovine calf serum (iron supplemented, Hyclone) and 0.5× antibiotic-antimycotic (Invitrogen). Cultures were maintained in 37°C/5% CO_2 humidified incubator. When necessary, cytosine-arabinofuranoside (Sigma) was added at 6 μM to inhibit glial growth.

Neurons were used between DIV 7 and 18. At least 1 day before experiments, two-thirds of the medium was replaced with fresh medium without glia inhibitor and antibiotics.

HEK293 Cell Culture and DNA Transfection

HEK293 cells were grown in DMEM (GIBCO) medium supplemented with 10% FBS and 1% Glutamax at 37°C in a humidified atmosphere of 5% CO_2, 95% air. NALCN cDNA used for the transfection was constructed from a rat clone (Lee et al., 1999) in a pTracer-CMV based vector, with 44 bp from the *Xenopus* β-globin sequence inserted into the 5′UTR. Clones were sequenced to ensure that only the ones with correct sequence were used. A similar construct encoding the human NALCN (99% amino acid identity with the rat ortholog) was also used for some experiments. No functional difference was observed between the two orthologs. Site-directed mutagenesis on the rat form NALCN was used to generate the EEKA mutant used in Figure 3. An EEEE mutant was also constructed, but this mutant did not generate measurable current. Lipofectamine 2000 (Invitrogen) was used as the transfection reagent for both the HEK293 cells and neurons. Neurons of ages of DIV 5–7 were used for transfection, and patch-clamp recordings were performed 48–60 hr later. Transfected cells were identified by the green fluorescence protein encoded in the same vector.

Patch-Clamp Analyses Using HEK293 Cells

All experiments were carried out at room temperature (20–25°C). Whole-cell currents were recorded 48–72 hr after transfection. Unless otherwise stated, pipette solution contained the following (in mM): 150 Cs, 120 Mes, 10 NaCl, 10 EGTA, 2 Mg_2ATP, and 10 HEPES (pH 7.4, Osm ~300 mOsm/L). Bath solutions contained 150 NaCl, 3.5 KCl, 2 $MgCl_2$, 1.2 $CaCl_2$, 10 HEPES, and 20 glucose (pH 7.4 with 5 mM NaOH, Osm ~330 mOsm/L). In the 0 Na^+, 0 K^+ bath, Na^+ and K^+ were replaced by $Tris^+$ or $NMDG^+$.

For selectivity measurement, the pipette solution contained 155 Cs, 120 Mes, 10 Cl, 10 EGTA, 2 Mg_2ATP, and 20 HEPES (pH 7.4, Osm ~300 mOsm/L). Bath contained 155 Na, 150 Cl, 10 HEPES, and 20 glucose (pH 7.4, Osm = 320 mOsm/L). NaCl was isotonically replaced with KCl and $CaCl_2$ for the measurements of P_{Na}/P_{Cs} and P_{Ca}/P_{Cs}, respectively. In the 10 Cl^--containing bath, Cl^- was replaced with Mes^-. The following equation was used to calculate the relative permeabilities of Na^+ and K^+ to Cs^+ (Hille, 2001).

$$P_X/P_{Cs} = [Cs]_i \exp(E_{rev}F/RT)/[X]_o \quad (1)$$

where E_{rev}, F, R, and T are the reversal potential, Faraday constant, gas constant, and absolute temperature, respectively. The relative Ca^{2+} permeability was calculated as

$$P_{Ca}/P_{Cs} = \gamma_{Cs}[Cs]_i \exp(E_{rev}F/RT)[\exp(E_{rev}F/RT)+1]/4\,\gamma_{Ca}[Ca]_o \quad (2)$$

where $\gamma_{Cs} = 0.70$ and $\gamma_{Ca} = 0.331$ are the activity coefficients (Hille, 2001).

Because of the "leakiness" of NALCN, special attention was taken to ensure that the currents recorded were from NALCN channel instead of nonspecific leaks from cell damage or loose seals. In the end of recording, either cation ion replacement (with $NMDG^+$ or $Tris^+$) or blocker (1 mM verapamil) application was used to assure that only cells with a tight seal were used for analysis.

One concern was that the currents we recorded might be a result of upregulation of other cation channels, especially some of the 28 TRP channels. The overall properties of I_{NALCN}, however, made it highly unlikely. First, most of the TRP channels have rectifying I-V relationships in the presence of ~mM $[Ca^{2+}]_o$ (Clapham, 2003; Owsianik et al., 2006; Ramsey et al., 2006). Among the TRPs that have a nearly linear I-V curve, they are either almost impermeable to Ca^{2+} (TRPM4 and TRPM5, activated by Ca^{2+}) or are much more selective for Ca^{2+} (P_{Ca}/P_{Na} ~1.0 or larger; TRPM2, M3, P3, P1+P2) than NALCN (P_{Ca}/P_{Na} = 0.38) (Clapham, 2003; Owsianik et al., 2006; Ramsey et al., 2006). Second, most of the TRPs are activated by stimuli such as Ca^{2+}, ADP-ribose, temperature, and receptors; NALCN is instantaneously active upon break-in (data not shown). Third, I_{NALCN} is not affected by $[Ca^{2+}]_i$ up to 1 mM or as low as a few nM (data not shown); many of the TRPs are inactivated by low (<10 nM) or high (>1 μM) $[Ca^{2+}]_i$ (Clapham, 2003; Owsianik et al., 2006; Ramsey et al., 2006). While these differences clearly separate the currents generated by TRPs and by NALCN, several TRPs (especially the TRPs that are believed to be intracellular) have not been characterized in detail, and we cannot exclude the possibility that they may generate currents of biophysical and pharmacological properties similar to those of I_{NALCN}.

Patch-Clamp Analysis Using Hippocampal Neurons

All experiments were carried out at room temperature (20–25°C) with cultured hippocampal neurons, except that Ca_V currents were recorded using acutely dissociated neurons. Pyramidal neurons were morphologically identified. For Na_V current recording, pipette solution contained the following (in mM): 145 CsAsp, 5 NaCl, 5 KCl, 2 $MgCl_2$, 10 EGTA, and 10 HEPES (pH 7.3, 315 mOsm/L). Bath contained the following: 50 NaCl, 5 $MgCl_2$, 1 $CaCl_2$, 2 $CoCl_2$, 10 TEA-Cl, 20 glucose, 145 sucrose, and 10 HEPES (pH7.4, 330 mOsm/L). For Ca_V current recordings, pipette solution contained the following (in mM): 115 CsAsp, 5 $MgCl_2$, 10 EGTA, 20 HEPES, 4 Mg-ATP, 0.3 Tris-GTP, and 14 phosphocreatine (di-tris salt) (pH 7.4; 277 mOsm/L). Bath solution contained the following (in mM): 155 TEA-Cl, 10 $BaCl_2$, 3.5 KCl, 1 $MgCl_2$, 10 HEPES, 10 glucose, and 10 sucrose (pH 7.4, 311 mOsm/L).

For voltage clamp used in recording the background leak Na^+ currents (Raman et al., 2000; Simasko, 1994), pipette solution contained the following (in mM): 10 NaCl, 12 KCl, 59 K_2SO_4, 4 MgCl2, 10 HEPES, 5 Tris-OH, 14 Tris-creatine phosphate, 4 Mg-ATP, and 0.3 Tris-GTP (pH 7.4, Osm ~300 mOsm/L). The 140 mM Na^+ bath contained the following (in mM): 140 NaCl, 5 KCl, 2 $CaCl_2$, 1 $MgCl_2$, 6 glucose, 10 HEPES, 2 CsCl, and 1 μM TTX (pH 7.4 with 2 Tris-OH, Osm ~315 mOsm/L). Tris-Cl was used to replace 126 mM NaCl in the 14 mM Na^+-containing bath. Because of the small sizes (~15 pA) of the leak Na^+ currents, special precaution was taken to ensure that the current was not a result of recording instability. After recording in a bath containing different $[Na^+]_o$, each recording was finished with the bath returning to the original Na^+ concentration. For nontransfected neurons, only those with a difference <5 pA between holding currents in the first and the last baths were used for further analysis. For the transfected ones, which had larger $I_{L\text{-}Na}$, baseline fluctuation of 20% of $\Delta I_{L\text{-}Na}$ was allowed in cell selection. Initial experiments comparing $\Delta I_{L\text{-}Na}$ in the WT and mutant neurons were done in a blinded fashion, in which the experimentalist did not know the genotype of the cells during the experiments.

For current-clamp recordings, pipette solution contained the following (in mM): 135 K-Asp, 5 NaCl, 5 KCl, 2 $MgCl_2$, 1 EGTA, 10 HEPES, 4 Mg-ATP, 0.3 Tris-GTP, and 14 phosphocreatine (di-tris) (pH adjusted to 7.2 with KOH, total K^+ about 147 mM). Bath solution contained the following (in mM): 150 NaCl, 3.5 KCl, 2 $MgCl_2$, 1.2 $CaCl_2$, 10 HEPES, and 20 glucose (pH 7.4 with 5 NaOH, Osm ~320 mOsm/L). Neurons were isolated with APV (10 μM), bicuculline (20 μM), and CNQX (20 μM). Currents (WT, +1.6 ± 0.9 pA, n = 18; mutant, +9.2 ± 3.8 pA, n = 15) were injected to elicit firing (Figures 7C and 7D). Some of the neurons cultured from both the WT and mutant showed spontaneous firing at 0 holding current.

Patch-clamp recordings were performed with an Axopatch-200A amplifier controlled by pClamp 9.2 software (Axon). Signals were filtered at 5 KHz and digitized at 10–20 kHz with a Digidata 1322A digitizer. Liquid junction potentials ≥5 mV (calculated with pClamp 9.2) were corrected.

ACKNOWLEDGMENTS

We thank Igor Medina, Alexander Jackson, and Margie Maronski for help on neuronal culture; Dr. Edward Perez-Reyes for the rat NALCN clone; Joshua Bradner and Dr. Eric Weinberg for pilot experiments in

the zebrafish; Dr. Jean Richa for ES cell injection; Drs. Bruce Bean, Francisco Bezanilla, David Clapham, Carol Deustch, Igor Medina, Betsy Navarro, Marc Schmidt, and Haoxing Xu for critically reading earlier versions of the manuscript. The initial investigation of NALCN and construction of vectors for the mutant were carried out in the laboratory of Dr. Clapham (Howard Hughes Medical Institute/Children's Hospital Boston, Harvard Medical School), who also kindly donated the amplifiers for the recordings. This work was supported in part by funding from the American Heart Association and the University of Pennsylvania Research Foundation.

Received: October 3, 2006
Revised: December 4, 2006
Accepted: February 2, 2007
Published: April 19, 2007

REFERENCES

Atherton, J.F., and Bevan, M.D. (2005). Ionic mechanisms underlying autonomous action potential generation in the somata and dendrites of GABAergic substantia nigra pars reticulata neurons in vitro. J. Neurosci. *25*, 8272–8281.

Bargmann, C.I. (1998). Neurobiology of the Caenorhabditis elegans genome. Science *282*, 2028–2033.

Bezanilla, F. (2000). The voltage sensor in voltage-dependent ion channels. Physiol. Rev. *80*, 555–592.

Catterall, W.A. (2000). From ionic currents to molecular mechanisms: the structure and function of voltage-gated sodium channels. Neuron *26*, 13–25.

Clapham, D.E. (2003). TRP channels as cellular sensors. Nature *426*, 517–524.

Crill, W.E. (1996). Persistent sodium current in mammalian central neurons. Annu. Rev. Physiol. *58*, 349–362.

Di Pasquale, E., Tell, F., Monteau, R., and Hilaire, G. (1996). Perinatal developmental changes in respiratory activity of medullary and spinal neurons: an in vitro study on fetal and newborn rats. Brain Res. Dev. Brain Res. *91*, 121–130.

Doyle, D.A., Morais Cabral, J., Pfuetzner, R.A., Kuo, A., Gulbis, J.M., Cohen, S.L., Chait, B.T., and MacKinnon, R. (1998). The structure of the potassium channel: molecular basis of K+ conduction and selectivity. Science *280*, 69–77.

Eggermann, E., Bayer, L., Serafin, M., Saint-Mleux, B., Bernheim, L., Machard, D., Jones, B.E., and Muhlethaler, M. (2003). The wake-promoting hypocretin-orexin neurons are in an intrinsic state of membrane depolarization. J. Neurosci. *23*, 1557–1562.

Feldman, J.L., Mitchell, G.S., and Nattie, E.E. (2003). Breathing: rhythmicity, plasticity, chemosensitivity. Annu. Rev. Neurosci. *26*, 239–266.

Franks, C.J., Pemberton, D., Vinogradova, I., Cook, A., Walker, R.J., and Holden-Dye, L. (2002). Ionic basis of the resting membrane potential and action potential in the pharyngeal muscle of Caenorhabditis elegans. J. Neurophysiol. *87*, 954–961.

Goldin, A.L. (2002). Evolution of voltage-gated Na(+) channels. J. Exp. Biol. *205*, 575–584.

Goldstein, S.A., Bayliss, D.A., Kim, D., Lesage, F., Plant, L.D., and Rajan, S. (2005). International Union of Pharmacology. LV. Nomenclature and molecular relationships of two-P potassium channels. Pharmacol. Rev. *57*, 527–540.

Heinemann, S.H., Terlau, H., Stuhmer, W., Imoto, K., and Numa, S. (1992). Calcium channel characteristics conferred on the sodium channel by single mutations. Nature *356*, 441–443.

Heurteaux, C., Guy, N., Laigle, C., Blondeau, N., Duprat, F., Mazzuca, M., Lang-Lazdunski, L., Widmann, C., Zanzouri, M., Romey, G., and Lazdunski, M. (2004). TREK-1, a K(+) channel involved in neuroprotection and general anesthesia. EMBO J. *23*, 2684–2695.

Hille, B. (2001). Ion Channels of Excitable Membranes, Third Edition (Sunderland, MA: Sinauer Associates, Inc.).

Hodgkin, A.L., and Katz, B. (1949). The effect of sodium ions on the electrical activity of the giant axon of the squid. J. Physiol. *108*, 37–77.

Horn, R. (2002). Coupled movements in voltage-gated ion channels. J. Gen. Physiol. *120*, 449–453.

Jackson, A.C., Yao, G.L., and Bean, B.P. (2004). Mechanism of spontaneous firing in dorsomedial suprachiasmatic nucleus neurons. J. Neurosci. *24*, 7985–7998.

Jones, S.W. (1989). On the resting potential of isolated frog sympathetic neurons. Neuron *3*, 153–161.

Kim, M.S., Morii, T., Sun, L.X., Imoto, K., and Mori, Y. (1993). Structural determinants of ion selectivity in brain calcium channel. FEBS Lett. *318*, 145–148.

Krishnan, K.S., and Nash, H.A. (1990). A genetic study of the anesthetic response: mutants of Drosophila melanogaster altered in sensitivity to halothane. Proc. Natl. Acad. Sci. USA *87*, 8632–8636.

Lear, B.C., Lin, J.M., Keath, J.R., McGill, J.J., Raman, I.M., and Allada, R. (2005). The ion channel narrow abdomen is critical for neural output of the Drosophila circadian pacemaker. Neuron *48*, 965–976.

Lee, J.H., Cribbs, L.L., and Perez-Reyes, E. (1999). Cloning of a novel four repeat protein related to voltage-gated sodium and calcium channels. FEBS Lett. *445*, 231–236.

Littleton, J.T., and Ganetzky, B. (2000). Ion channels and synaptic organization: analysis of the *Drosophila* genome. Neuron *26*, 35–43.

Mir, B., Iyer, S., Ramaswami, M., and Krishnan, K.S. (1997). A genetic and mosaic analysis of a locus involved in the anesthesia response of Drosophila melanogaster. Genetics *147*, 701–712.

Nash, H.A., Scott, R.L., Lear, B.C., and Allada, R. (2002). An unusual cation channel mediates photic control of locomotion in *Drosophila*. Curr. Biol. *12*, 2152–2158.

Nicholls, J.G., Martin, A.R., Wallace, B.G., and Fuchs, P.A. (2001). From Neuron to Brain, Fourth Edition (Sunderland, MA: Sinauer Associates Inc.).

Nilius, B., Voets, T., and Peters, J. (2005). TRP channels in disease. Sci. STKE *2005*, re8. 10.1126/stke.2952005re8.

Owsianik, G., Talavera, K., Voets, T., and Nilius, B. (2006). Permeation and selectivity of TRP channels. Annu. Rev. Physiol. *68*, 685–717.

Pena, F., and Ramirez, J.M. (2004). Substance P-mediated modulation of pacemaker properties in the mammalian respiratory network. J. Neurosci. *24*, 7549–7556.

Raman, I.M., and Bean, B.P. (1997). Resurgent sodium current and action potential formation in dissociated cerebellar Purkinje neurons. J. Neurosci. *17*, 4517–4526.

Raman, I.M., Gustafson, A.E., and Padgett, D. (2000). Ionic currents and spontaneous firing in neurons isolated from the cerebellar nuclei. J. Neurosci. *20*, 9004–9016.

Ramsey, I.S., Delling, M., and Clapham, D.E. (2006). An introduction to TRP channels. Annu. Rev. Physiol. *68*, 619–647.

Robinson, R.B., and Siegelbaum, S.A. (2003). Hyperpolarization-activated cation currents: from molecules to physiological function. Annu. Rev. Physiol. *65*, 453–480.

Sather, W.A., and McCleskey, E.W. (2003). Permeation and selectivity in calcium channels. Annu. Rev. Physiol. *65*, 133–159.

Simasko, S.M. (1994). A background sodium conductance is necessary for spontaneous depolarizations in rat pituitary cell line GH3. Am. J. Physiol. *266*, C709–C719.

Strohl, K.P. (2003). Periodic breathing and genetics. Respir. Physiol. Neurobiol. *135*, 179–185.

Tang, S., Mikala, G., Bahinski, A., Yatani, A., Varadi, G., and Schwartz, A. (1993). Molecular localization of ion selectivity sites within the pore of a human L-type cardiac calcium channel. J. Biol. Chem. *268*, 13026–13029.

van Swinderen, B. (2006). A succession of anesthetic endpoints in the Drosophila brain. J. Neurobiol. *66*, 1195–1211.

Viemari, J.C., Burnet, H., Bevengut, M., and Hilaire, G. (2003). Perinatal maturation of the mouse respiratory rhythm-generator: in vivo and in vitro studies. Eur. J. Neurosci. *17*, 1233–1244.

Yang, X.C., and Sachs, F. (1989). Block of stretch-activated ion channels in Xenopus oocytes by gadolinium and calcium ions. Science *243*, 1068–1071.

Yang, J., Ellinor, P.T., Sather, W.A., Zhang, J.F., and Tsien, R.W. (1993). Molecular determinants of Ca2+ selectivity and ion permeation in L-type Ca2+ channels. Nature *366*, 158–161.

Yu, F.H., and Catterall, W.A. (2004). The VGL-chanome: a protein superfamily specialized for electrical signaling and ionic homeostasis. Sci. STKE *2004*, re15. 10.1126/stke.2532004re15.